JOURNAL OF SOLID STATE CHEMISTRY 56, 116–121 (1985)

# Mössbauer Emission Spectroscopy in $La_2NiO_4$

J. FONTCUBERTA*

*Facultat Física, Universitat de Barcelona, Diagonal 645, Barcelona 28, Catalunya, Spain*

AND J. B. GOODENOUGH

*Inorganic Chemistry Laboratory, South Parks Road, Oxford OX1 3QR, England*

Received April 9, 1984; in revised form July 11, 1984

Mössbauer spectra of $^{57}Co:La_2NiO_4$ have been measured at 297, 77, and 4.2 K. The spectra show at least three inequivalent positions for the $^{57}Co^{3+}$ impurity. The existence of a uniquely charged $^{57}Fe^{3+}$ daughter is discussed in terms of the band structure of this oxide. A mixed $^{57}Fe^{3+}$, $^{57}Fe^{4+}$ daughter state is predicted for *p*-type $^{57}Co:La_2Li_{1/2}Co_{1/2}O_4$. © 1985 Academic Press, Inc.

## Introduction

Nuclear transformations in solids provide probes for the study of the microscopic properties of materials. In particular, the phenomena that occur after nuclear decay depend on the local environment of the radioactive species (*1*), and it has recently been shown that these phenomena are also sensitive to the character and concentration of defects existing in a solid at some distance from the decaying nucleus (*2*).

In this paper we consider the transformation by electron capture of $^{57}Co$ into $^{57}Fe$ at a cobalt substitutional impurity in $La_2NiO_4$. Removal of the captured electron from an inner shell gives rise to an electron-vacancy cascade, which generates in turn an Auger-electron cascade. The 14.4-keV $\gamma$-ray radiation from the $^{57}Fe^{m+}$ daughter nucleus can be analyzed by Mössbauer spectroscopy; the Mössbauer spectrum reveals the environment of the $^{57}Co$-atom probe about $10^{-7}$ sec after its decay.

As a result of the Auger cascade, electrons are ejected from the probe atom. If these electrons are not recaptured in a time $\tau < 10^{-7}$ sec, the probe atom exhibits the Mössbauer spectrum of a more positive state. In $^{57}CoO$, for example, both $Fe^{2+}$ and $Fe^{3+}$ ions have been obtained from $^{57}Co^{2+}$ (*3*). However, no charge states higher than $Fe^{3+}$ have ever been observed for the iron daughter (*4*) despite stabilization of octahedrally coordinated $Fe^{4+}$ ions in the perovskites $CaFeO_3$ and $SrFeO_3$ (*5*) as well as in the tetragonal compound $La_{3/2}Sr_{1/2}Li_{1/2}Fe_{1/2}O_4$ (*6*), which has $Li^+$ and $Fe^{4+}$ ions ordered in the perovskite layers of the $K_2NiF_4$ structure.

$La_2NiO_4$ is an oxide with the tetragonal

*To whom correspondence should be addressed.

0022-4596/85 $3.00

$K_2NiF_4$ structure. This structure consists of alternating perovskite and rock salt layers; these are $LaNiO_3$ and LaO layers in $La_2NiO_4$. Whether antiferromagnetic order or a charge-density wave is stabilized at lowest temperatures has been addressed elsewhere (*7–9*).

In the case of $La_2NiO_4$, a tolerance factor $t = R_{AO}/\sqrt{2}R_{BO} < 1$, where $R_{AO}$ is the sum of the $La^{3+}$ and $O^{2-}$ ionic radii and $R_{BO}$ is the sum of the $Ni^{2+}$ and $O^{2-}$ ionic radii, introduces a stretching of the La–O bond and a compression of the Ni–O bond. The Ni–O–Ni distance is about 8% shorter in $La_2NiO_4$ than in NiO. This compression appears to transform the $d_{x^2-y^2}$ orbitals, which are directed toward basal-plane $O^{2-}$ ions, into itinerant-electron orbitals of a narrow $\sigma^*_{x^2-y^2}$ band; the $d_{z^2}$ orbitals directed toward *c*-axis nearest neighbors remain strongly correlated (*7*).

At high temperatures $La_2NiO_4$ exhibits a Curie–Weiss law having a Curie constant typical of that for an $S = 1$ state at octahedral-site $Ni^{2+}$ ions. However, below 200 K there is a smooth change to an apparent Curie–Weiss law having a Curie constant more typical of an $S = 1/2$ state. This change suggested that, rather than long-range antiferromagnetic order at low temperatures, there was a decoupling of the itinerant $\sigma^*_{x^2-y^2}$ electrons from the localized $d_{z^2}$ electrons via formation of a charge-density wave in the $\sigma^*_{x^2-y^2}$ band (*8*). (Alternatively the change could signal a disproportionation into an ordered array of high-spin and low-spin trivalent Ni.)

In a previous publication (*9*), the Mössbauer spectroscopy of $^{57}Fe$-doped and $^{57}Co$-doped $La_2NiO_4$ have been reported for $T =$ 4.2, 77, and 297 K. The samples were *p*-type and contained inhomogeneous intergrowths consisting of several consecutive $LaNiO_3$ perovskite layers. In these samples there was direct evidence from the Mössbauer spectra of antiferromagnetic order at 4.2 K, but the data were not inconsistent with the formation of a charge-density wave in homogeneous, stoichiometric $La_2NiO_4$. In both source and absorber experiments, $^{57}Fe^{3+}$ was observed over the entire temperature range $4.2 < T < 300$ K.

An analysis of the factors that determine the charge state of the $^{57}Fe$ daughter ion is presented in this paper. The analysis has general applicability, and the appearance in $^{57}Co:La_2NiO_4$ of a unique $^{57}Fe^{3+}$ charge state after nuclear decay is satisfactorily explained.

## Sample Preparation

$La_2NiO_4$ was prepared by mixing the appropriate amounts of the corresponding oxides followed by systematic grinding and firing at 1200°C in air (*9*). A sintered pellet of the single-phase product was made active by dropping a $^{57}CoCl$ solution on its surface and heating until dry. Diffusion of the $^{57}Co$ into the sample was carried out at 1150°C for 48 hr. The sample was cooled down slowly inside the furnace, and any surface activity remaining was removed by cleaning the pellet with dilute HCl. The final activity of the sample was about 4 mCi. A nonactive sample was synthesized together with the active one to permit a check of the structure of the final compound.

The X-ray powder patterns at room temperature were recorded on a conventional Philips diffractometer using Cu$K\alpha$ radiation. Cell constants were refined with a least-squares program (AFFMA) on the basis of the tetragonal $K_2NiF_4$ structure (*I*/*4mmm*) by using 39 reflections ($K\alpha_1$, $K\alpha_2$) up to 100° ($2\theta$). The lattice parameters obtained from the fitting, $a = 3.867(1)$ Å and $c = 12.665(6)$ Å, are in good agreement with those previously reported (*7, 8*).

## Mössbauer Spectra

The Mössbauer spectra were taken with a constant-acceleration drive system and a

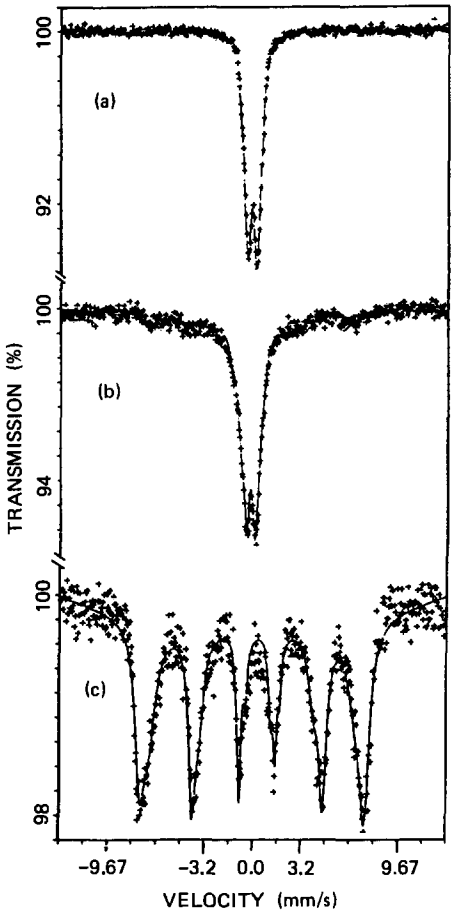


FIG. 1. Mössbauer emission spectra of $^{57}Co:La_2NiO_4$ at temperatures (a) 297 K, (b) 77 K, (c) 4.2 K.

multichannel analyzer. A thin PdFe foil was used as absorber; it has an isomer shift $\delta$ = 0.1749 mm/sec. (All line shifts are given with respect to $\alpha$-Fe at room temperature.) In the figures, positive velocity indicates that source and absorber move toward one another.

The source was placed inside a cryostat, and the Mössbauer spectra were taken at 297, 77, and 4.2 K. Where the magnetic hyperfine spectrum appeared ($T < 77$ K), it proved necessary to use a large magnetic-field distribution to get a reasonably accurate fit to the data. In that case, the natural linewidth was assumed for each component.

Figure 1 shows the spectra of $^{57}Co:La_2NiO_4$. Table I summarizes the relevant Mössbauer parameters obtained from the fit. The three different isomer shifts and quadrupole splittings correspond to $^{57}Fe^{3+}$ ions substituting for nickel in three different structural locations (*9*). In this paper we focus attention on the $^{57}Fe^{3+}$ charge state of the probe-ion daughter.

## Discussion

### *A. Energy Diagram*

Any discussion of possible valence states must begin with an energy diagram. The construction of energy diagrams for oxides has been discussed extensively elsewhere (*10*).

In $La_2NiO_4$, as in other transition-metal oxides, the top of the $O^{2-}$-ion $2p^6$ band and the bottom of the rare-earth $5d,6s$ and transition-metal $4s$ bands are separated by a large (>4 eV) energy gap. Since the lanthanum $4f^1$ level lies above the lanthanum $5d,6s$ band edge, the only remaining problem is the placement of the $Ni^{3+/2+}:3d^8$ band relative to the top of the $O^{2+}$-ion $2p^6$ band. If the Fermi energy $E_F$ lies above this band edge, then the formal valences provide a correct count of the total number of 3d electrons per nickel atom.

In NiO the top of the narrow $Ni^{3+/2+}:3d^8$ band has been located about 1.4 eV above the top of the $O^{2-}$-ion $2p^6$ band and about 3 eV below the bottom of the $Ni^{2+/+}:3d^9$ band (*11*). The splitting between $3d^8$ and $3d^9$ levels is due to strong correlations among the nickel $e_g$ electrons, which carry a spontaneous atomic moment ($S = 1$). In $La_2NiO_4$, compression of the Ni–O–Ni distance within a basal plane enhances the interactions between $d_{x^2-y^2}$ orbitals, which are directed toward basal-plane $O^{2-}$-ion near neighbors, and a narrow $\sigma^*_{x^2-y^2}$ band of itin-

TABLE I

PARAMETERS OBTAINED FROM MÖSSBAUER EMISSION SPECTRA MEASURED AT TEMPERATURES OF 297, 77, and 4.2 K WITH A PdFe ABSORBER

| $T$ (K) | IS (mm/sec) | EQ (mm/sec) | HF (kOe) | DHF (kOe) | $\Gamma$ (mm/sec) | % | CHI |
|---|---|---|---|---|---|---|---|
| 297 | 0.23(1) | 1.30(2) | | | 0.50(6) | 38(8) | 1.19 |
| | 0.25(2) | 0.86(4) | | | 0.29(7) | 17(10) | |
| | 0.23(1) | 0.44(1) | | | 0.41(2) | 45(7) | |
| 77 | 0.47(3) | 1.28(4) | | | 1.1(2) | 35(3) | 1.03 |
| | 0.35(1) | 0.69(2) | | | 0.64(2) | 39(10) | |
| | 0.23(16) | −0.2(1) | 395 | 51 | 0.20 | 20(6) | |
| | 0.15(22) | 0 | 170 | 26 | 0.20 | 6(4) | |
| 4.2 | 0.32(8) | 1.9(5) | | | 1.6(5) | 11(7) | 1.09 |
| | 0.34(3) | −0.19(2) | 467 | 49 | 0.20 | 24(4) | |
| | 0.34(4) | −0.12(2) | 435 | 38 | 0.20 | 65(2) | |

*Note.* IS, EQ, and $\Gamma$ are the isomer shift, quadrupole splitting, and linewidth (in mm/sec). DHF is the standard deviation of a Gaussian distribution of magnetic fields. This IS is referred to room-temperature metallic iron. The % is the percentage of the total area, CHI is the $\chi^2$ value of the fit. The figures quoted in parentheses denote the estimated errors of the fitted parameters and refer to the last significant figure.

erant-electron states is formed from the $d_{x^2-y^2}$ parentage. The width of the $\sigma^*_{x^2-y^2}$ band appears to be comparable to the correlation splitting, so any correlation splitting of the half-filled $\sigma^*_{x^2-y^2}$ band can only produce, at most, a small bandgap. On the other hand, there is no compression of the Ni–O distance along the $c$-axis, so the $d_{z^2}$ electrons remain strongly correlated, and the $d^1_{z^2}$ state lies below $E_F$ split by 2–3 eV from an empty $d^2_{z^2}$ energy located above $E_F$. The filled nickel $t_2^6$ manifold lies well below $E_F$. Therefore the energy diagram for homogeneous, stoichiometric $La_2NiO_4$ can be represented by Fig. 2a. Compression of the Ni–O bond in the basal plane should raise the center of the $\sigma^*_{x^2-y^2}$ band relative to the top of the $O^{2-}$-ion $2p^6$ band, so $E_F$ can be placed unambiguously above the top of the $O^{2-}$-ion $2p^6$ band in $La_2NiO_4$.

The $La_2NiO_4$ normally prepared is neither homogeneous nor stoichiometric. It tends to be $p$-type, and the presence of $Ni^{3+}$ ions can be directly observed by iodometric titration (*7*). Electron microscopy has also provided direct evidence for some perovskite intergrowths, introduced at random, that are multiple (in contrast to a single) $LaNiO_3$ perovskite layers between two rock salt LaO layers (*12*). The perovskite $LaNiO_3$ is metallic; the stronger covalence with low-spin $Ni^{III}$ ions transforms the $\sigma$-antibonding orbitals of $e_g$ parentage into a

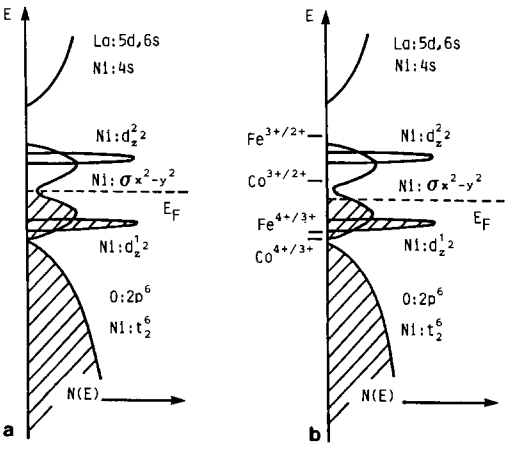


FIG. 2. Schematic energy-band diagram for (a) stoichiometric, homogeneous $La_2NiO_4$ and (b) Fe- and Co-doped $La_2NiO_4$.

narrow $\sigma^*$ band of itinerant one-electron states that are only weakly correlated (*10*). Electron transfer from the $La_2NiO_4$ regions to the $LaNiO_3$ layers would lower $E_F$ below the middle of the $\sigma^*_{x^2-y^2}$ band of the $La_2NiO_4$ regions even if most of the $Ni^{3+}$ ions are trapped in the perovskite layers.

Any nickel-ion vacancies would also tend to trap two *d*-band holes as $Ni^{III}$ ions at near-neighbor nickel atoms. In NiO, the acceptor levels associated with a cation vacancy are about 0.6 and 0.8 eV above the top of the $Ni^{3+/2+}: 3d^8$ band (*10*); in $La_2NiO_4$, the greater separation of nickel nearest neighbors and the greater screening by itinerant $\sigma^*_{x^2-y^2}$ electrons would reduce this energy to about 0.2–0.4 eV above $E_F$.

Substitutional Co impurities would have a $Co^{3+/2+}: 3d^7$ redox energy at least 0.5 eV above $E_F$ as a result of the smaller effective nuclear charge experienced by 3*d* electrons on the lighter cobalt atom (*10*). Therefore a $^{57}Co$ impurity could not exist as a $^{57}Co^{2+}$ ground-state species; such a species would lose an electron to the nickel $\sigma^*_{x^2-y^2}$ or $d_{z^2}$ bands to become $^{57}Co^{3+}$. It is not possible to predict the spin state of the $^{57}Co^{3+}$ species from these semiempirical arguments. An energy diagram for our $^{57}Co: La_2NiO_4$ is illustrated in Fig. 2b. Electron correlations at the impurity center are strong enough to inhibit the formation of $^{57}Co^{4+}$ ions.

These arguments are consistent with independent empirical evidence from other systems. The spinel $Co_2NiO_4$, for example, exhibits an equilibrium between the two configurations

$$Co^{2+}[Ni^{3+}Co^{III}]O_4 \rightleftharpoons Co^{3+}[Ni^{2+}Co^{III}]O_4$$

where $Co^{III}$ represents a low-spin $t_{2}^{6}e^{0}$ configuration. In this compound, low-spin $Co^{III}$ is stable in the presence of a mixed $Ni^{3+/2+}$ valence on the same subarray of octahedral sites (*13*). Moreover, in the perovskite system $La(Ni_{1-x}Co_x)O_3$, the low-spin $Ni^{III}$ and $Co^{III}$ ions coexist on the same subarray of octahedral sites with no evidence of any further oxidation of the $Co^{III}$ ions by the $Ni^{III}$ ions (*14, 15*).

Since Fe is to the left of Co in the Periodic Table, a similar argument leads to the prediction that $^{57}Fe$ impurities can only exist as $^{57}Fe^{3+}$ ions in $La_2NiO_4$. In fact, only $Fe^{3+}$-ion Mössbauer spectra were observed in $^{57}Fe: La_2NiO_4$ (*9*). This deduction is also consistent with the observation of only $Fe^{3+}$ ions in the perovskite systems La $(Ni_{1-x}Fe_x)O_3$ and $La(Fe_{1-x}Co_x)O_3$ (*15, 16*).

### *B. $^{57}Fe$ Daughters in $^{57}Co: La_2NiO_4$*

The fact that $^{57}Co$ and $^{57}Fe$ are expected to enter $La_2NiO_4$ as $^{57}Co^{3+}$ and $^{57}Fe^{3+}$ still leaves open the question whether the Mössbauer spectrum from the daughters of electron capture by $^{57}Co^{3+}$ in $La_2NiO_4$ are uniquely $^{57}Fe^{3+}$ or may be mixed-valent $^{57}Fe^{3+}$ and $^{57}Fe^{4+}$. The possibility of mixed-valent $Fe^{3+}$, $Fe^{4+}$ daughters is suggested by the report of Demazeau *et al.* (*17*) that the ordered compound $^{57}Fe: La_2Li_{1/2}Co_{1/2}O_4$ gives both $Fe^{4+}$ and $Fe^{3+}$ Mössbauer spectra. However, no evidence of any $^{57}Fe^{4+}$ species was observed in our Mössbauer spectra of $^{57}Co: La_2NiO_4$ (see Table I). Details of the Mössbauer analysis are presented elsewhere (*9*).

Nuclear electron capture by a $^{57}Co^{3+}$ nucleus leads to an excited $^{57}Fe^{3+}$ ion, and excitation of an Auger electron from the $^{57}Fe^{3+}$ ion to the conduction band is possible. Moreover, electron decay from the conduction band need not be a return to the $^{57}Fe^{4+}$ ion; it has a greater probability of capture by the $\sigma^*_{x^2-y^2}$ band. The probabilities of electron-hole recombination at an iron atom and a nickel atom are

$$\lambda_{Fe} \sim \sigma_{Fe}[Fe],\ \lambda_{Ni} \sim \sigma_{Ni}[Ni]$$

where $\sigma_{Fe}$ and $\sigma_{Ni}$ are the capture cross sections of the $^{57}Fe^{4+}$ and the $Ni^{3+}$ centers, respectively. However, the $^{57}Fe^{4+}$ ion will capture an electron from the $\sigma^*_{x^2-y^2}$ band in a time shorter than $10^{-7}$ sec so long as the $Fe^{4+/3+}$ level lies below the Fermi energy $E_F$.

Independent measurement of the ESR spectra of $Fe:TiO_2$ and $Ni:TiO_2$ have shown that the $Fe^{4+/3+}$ level lies some 3 eV below the $Fe^{3+/2+}$ level and at least 1 eV below the $Ni^{3+/2+}$ levels (*18*). The large effective correlation splitting between the $Fe^{3+/2+}$ and $Fe^{4+/3+}$ levels arises from the fact that high-spin $Fe^{3+}$ ions have a half-filled $3d^5$ shell. Therefore, the observation of a unique $^{57}Fe^{3+}$ daughter ion in $La_2NiO_4$ follows at once from the model of Fig. 2b.

There remains to show that this argument is consistent with the Mössbauer data (*17*) for $^{57}Fe:La_2Li_{1/2}Co_{1/2}O_4$. In this latter compound the $Co^{3+}$ ions have only $Li^+$ cation near neighbors in the basal plane, so the $Co^{3+}:3d^7$ intermediate-spin configuration is localized. In this case there is no band of itinerant-*d*-electron states; the $Co^{4+/3+}$ and $Co^{3+/2+}$ redox energies are split from one another by correlation energies of several electron-volts. In such a case, any oxidation of $La_2Li_{1/2}Co_{1/2}O_4$ would lead to mixed $Co^{4+}$ and $Co^{3+}$ ions. Since the high-spin $Fe^{4+/3+}:3d^5$ energy appears to lie just above the low-spin $Co^{IV/III}:t_{2e}^6e^0$ energy, any holes tend to be captured by the $^{57}Fe$ impurities.

It follows that even slightly oxidized $^{57}Fe:La_2Li_{1/2}Co_{1/2}O_4$ may give a mixed $Fe^{3+}$, $Fe^{4+}$ Mössbauer spectrum. It also follows that a slightly oxidized $^{57}Co:La_2Li_{1/2}Co_{1/2}O_4$ should give a mixed $Fe^{3+}$, $Fe^{4+}$ Mössbauer spectrum from its daughter ions. Demonstration of this prediction would provide the first example of a $^{57}Fe^{4+}$-ion daughter.

## Acknowledgments

The authors are thankful to Dr. G. Longworth for his assistance in obtaining the low-temperature Mössbauer spectra. This work has been supported by the CIRIT (Generalitat de Catalunya).

## References

1. H. J. EMELÉUS (Consultant Ed.), "MTP-International Review of Science Radiochemistry," Vol. 8.
2. J. TEJADA AND F. PARAK, *Hyperfine Interact.* **10,** 1227 (1981); T. HARAMI, J. LOOCK, E. HUENGES, J. FONTCUBERTA, X. OBRADORS, J. TEJADA, AND F. PARAK, *J. Phys. Chem. Solids* **45,** 181 (1984).
3. G. K. WERTHEIM, *Phys. Rev.* **124,** 764 (1961).
4. J. G. MULLEN AND H. N. OK, *Phys. Rev.* **168,** 550 (1966).
5. P. K. GALLAGER, J. B. MACCHESNEY, AND D. N. E. BUCHANAN, *J. Chem. Phys.* **41,** 2429 (1964); Y. TAKEDA, S. NAKA, M. TAKANO, T. SHINJO, T. TAKADA, AND M. SHIMADA, *Mater. Res. Bull.* **12,** 923 (1977).
6. G. DEMAZEAU, M. POUCHARD, N. CHEVREAU, M. THOMAS, F. MÉNIL, AND P. HAGENMULLER, *Mater. Res. Bull.* **16,** 689 (1981); G. DEMAZEAU, B. BUFFAT, M. PUCHARD, AND P. HAGENMULLER, *J. Solid State Chem.* **45,** 88 (1982).
7. J. B. GOODENOUGH AND S. RAMASESHA, *Mater. Res. Bull.* **17,** 383 (1982).
8. K. K. SINGH, P. GANGULY, AND J. B. GOODENOUGH, *J. Solid State Chem.* **52,** 254 (1984).
9. J. FONTCUBERTA, G. LONGWORTH, AND J. B. GOODENOUGH, *Phys. Rev.*, in press.
10. J. B. GOODENOUGH, *Prog. Solid State Chem.* **5,** 145 (1971).
11. M. P. DARE-EDWARDS, J. B. GOODENOUGH, A. HAMNETT, AND N. D. NICHOLSON, *J. Chem. Soc., Faraday Trans. 2* **77,** 643 (1981).
12. J. DRENNAN, C. P. TAVARES, AND B. C. H. STEELE, *Mater. Res. Bull.* **17,** 621 (1982).
13. P. D. BATTLE, A. K. CHEETHAM, AND J. B. GOODENOUGH, *Mater. Res. Bull.* **14,** 1013 (1979).
14. K. ASAI, H. SEKIZAWA, K. MIZUSHIMA, AND S. IIDA, *J. Phys. Soc. Jpn.* **43,** 1093 (1977).
15. C. N. R. RAO, O. M. PARKASH, AND P. GANGULY, *J. Solid State Chem.* **15,** 186 (1975).
16. K. ASAI AND H. SEKIZAWA, *J. Phys. Colloq. (Orsay, Fr.)* **40,** 225 (1979).
17. G. DEMAZEAU, M. POUCHARD, M. THOMAS, J. F. COLOMBET, J. C. GRENIER, L. FOURNÉS, J. L. SOUBEYROUX, AND P. HAGENMULLER, *Mater. Res. Bull.* **15,** 451 (1980).
18. K. MIZUSHIMA, M. TANAKA, A. ASAI, S. IIDA, AND J. B. GOODENOUGH, *J. Phys. Chem. Solids* **40,** 1129 (1979).